Molecular-dynamics study of structural anisotropy and anelasticity in metallic glasses

T. Tomida* and T. Egami
Department of Materials Science and Engineering and Laboratory for Research on the Structure of Matter, University of Pennsylvania, Philadelphia, Pennsylvania 19104-6272
(Received 29 January 1993)

Molecular-dynamics simulations have been carried out to study the structural anisotropy in anelastically deformed glassy metals. Two model glass structures, a single-component glass of 4394 particles interacting via a modified Johnson potential and a two-component glass of 2048 particles with the Lennard-Jones potentials, were thermomechanically deformed below their glass-transition temperature. The structural anisotropy caused by anelastic deformation is dominated by the bond-orientational anisotropy (BOA) with a large sixth-order spherical-harmonic component in both model structures. The sixth-order BOA could be associated with the local bond-orientational order (BOO) of the basic local structural units, such as tetrahedral and icosahedral clusters. We propose a scheme to describe the structure of the glasses and their mechanical properties, based upon the sixth-order local BOO.

I. INTRODUCTION

Thermomechanical (creep) deformation in metallic glass has been the subject of numerous investigations and is still of much current interest.[1–6] Although these efforts have revealed many salient features involved in the deformation, the understanding of the phenomenon at a microscopic or atomic level has been severely hampered by the difficulty of characterizing the detailed structure of glasses. The purpose of this work is to introduce an atomistic description of the deformation of the glassy metals in terms of the higher-order bond-orientational anisotropy (BOA) and local bond-orientational order (BOO) using the molecular-dynamics simulation of creep deformation and to attempt to identify the mechanism of deformation in the glassy metals.

It is now well established in the study of viscous flow that there exists two distinct components in the viscous response during the creep deformation: anelasticity and viscoplasticity.[2] The anelasticity is characterized by time-dependent recovery of the deformation on unloading, while the viscoplasticity is, as the word implies, irreversible. On the other hand, a study of the effect of creep on magnetic properties has shown that the creep deformation of ferromagnetic metallic glasses results in the formation of uniaxial magnetic anisotropy.[2] What emerges by linking detailed investigations on such seemingly different properties is that the creep deformation not only gives rise to a homogeneous flow in the material, but also produces an anisotropy to its atomic structure that is closely or directly related to the mechanisms for both the mechanical deformation and the magnetic anisotropy. The indication of the induced structural anisotropy from the viscoelastic approach is the existence of the anelasticity. The recovery of shape under no external stress obviously requires an anisotropic structure involved which can be either localized or homogeneously distributed throughout the material. Argon and Kuo[3,4] proposed a flow model employing complexes consisting of 5–20 atoms that undergo a shear transformation, based on observation of bubble raft deformation,[5] and attributed the anelasticity to backward shear transformations of the complexes.[4] Subsequently, the shear transformation was observed in a two-dimensional computer simulation of the plastic shearing of glasses.[6] Although the authors did not refer to a particular anisotropy associated with the shear transformation, the theory and simulation automatically predict more or less homogeneously distributed structural anisotropy involved in the anelasticity. There had also been an argument on whether the origin is homogeneous or heterogeneous regarding the magnetic anisotropy[2,7–9] until Hilzinger's experiment.[9] Hilzinger[9] measured the creep-induced magnetic anisotropy in nearly zero-magnetostrictive samples and found that the direction of magnetically easy axis is not affected by the sign of magnetostriction, suggesting that its origin is not the heterogeneous internal stress distribution producing anisotropy via magnetostriction, but is the atomic-level structural anisotropy.

A successful attempt of a direct observation of the creep-induced structural anisotropy was made by Suzuki, Haimovich, and Egami.[10] The authors measured the x-ray-diffraction intensities for creep-deformed Fe-Ni-Si-B amorphous ribbons with the diffraction vectors parallel and perpendicular to the stress direction and concluded that the contrasting behaviors of the first and second peaks of the intensity are best explained by the BOA. The BOA describes the anisotropy in the distribution of the orientations of the atomic bonds defined by a pair of atoms which are the nearest neighbors to each other. As a result of creep deformation, the density of atomic bonds along the direction of the tensile stress was found to be smaller than along the perpendicular direction.

Hirsher, Egami, and Marinero[12] and Yan *et al.*[13] conducted similar experiments on Tb-Fe (Ref. 12) and Tb-Co-Fe (Ref. 13) sputter-deposited amorphous films and found the same anisotropy in the x-ray-scattering intensity. Yan *et al.*[13] suggested that the in-plane compressive stress and thermal activation due to incoming atoms onto the film surface during sputtering may provide a local environment quite similar to that under the creep and induce the BOA. However, further experimental investiga-

0163-1829/93/48(5)/3048(10)/$06.00 ©1993 The American Physical Society

tions have been frustrated by the complexity of the structure of the glass, which possesses no translational symmetry. The diffraction experiment at present has not provided direct information on the atomistic details of structural anisotropy.

A fruitful method to investigate how the stress affects the atomic rearrangement during annealing is a computer simulation such as molecular dynamics (MD). Although the computer simulation has a limitation on the number of particles and the time scale of the system being simulated, it provides a set of information in the system which should lead us to an intuitive picture linking experimental results. We present in this article two sets of the results of MD simulations of creep deformation below the glass-transition temperature (T_g) using a single-component glass with a modified Johnson potential[14] and a two-component, or binary-alloy, glass with a Lennard-Jones (LJ) potential. The results show that the predominant structural anisotropy caused by the creep deformation is the BOA with the $l=6$ spherical harmonic component, both in the single-component glass and in the alloy glass. Apparently a twofold stress activates a sixfold structural anisotropy. When the stress is removed, the anisotropy relaxes with a broad distribution of the activation energy, indicating that this anisotropy is directly related to anelasticity. The activation and relaxation of the BOA will be discussed in conjunction with a microscopic mechanism of the flow of the material.

II. COMPUTER MODEL OF CREEP DEFORMATION

A. Single-component glass with a modified Johnson potential

Employing a modified Johnson potential[14] that was originally developed for bcc iron,[15] a single-component glass consisting of 4394 particles, referred as the modified Johnson glass henceforth, was constructed. The integration time step for this simulation was set to be 10^{-15} sec, that is about 100th of the Debye time for this potential. Periodic boundary conditions were maintained on all six faces of the pseudocubic assembly.

Starting with the bcc structure, the assembly in a cubic block was equilibrated in a liquid state for 10 000 time steps at 3000 K. Then the assembly was cooled down to 700 K [the glass-transition temperature of a modified Johnson potential glass is approximately 900 K (Ref. 16)], for 2000 time steps. The pressure of the system during this procedure was maintained to be 0.02 eV/Å^3 by changing the size of the cubic block and linearly displacing all the atoms every 100 time steps, Thus using a pseudo-constant-pressure mode. The assembly was then relaxed at the same temperature for 5000 time steps keeping the pressure zero. In order to promote further relaxation and construct model glasses at several temperatures from 500 to 900 K, the system was quenched or heated by a rate of 1 K/step and maintained at those temperatures for 5000 time steps without any change of the boundary condition and therefore with the volume constant.

These model glasses were creep deformed at a temperature ranging from 500 to 900 K. The shear strains as described below were applied to the model structure every 100 time steps, so that the tensile stress along the z axis, σ_z, is kept constant, simulating creep deformation. Thus the boundary condition was not cubic, but orthorhombic during the creep deformation:

$$\varepsilon=\frac{1}{3}\begin{bmatrix}-\gamma & 0 & 0\\ 0 & -\gamma & 0\\ 0 & 0 & 2\gamma\end{bmatrix}. \tag{1}$$

Each deformation was performed by displacing every atom in accordance with the linear elastic displacement field corresponding to the strain.

B. Two-component glass with a Lennard-Jones potential

To simulate a two-component alloy glass, a mixture of LJ potential ($4\varepsilon[(\sigma/r)^6-(\sigma/r)^{12}]$) with different length parameters σ_{AA} and σ_{BB} was introduced. The length parameter for unlike pairs of particles was given by $\sigma^2_{AB}=(\sigma^2_{AA}+\sigma^2_{BB})/2$. The ratio of $\sigma^2_{AA}/\sigma^2_{BB}$ and the atomic concentration were chosen to be 0.8 and 0.5, respectively. The depths of these potentials were chosen by the ratio $\varepsilon_{AA}:\varepsilon_{BB}:\varepsilon_{AB}=1:1/0.9:1/0.8$ to alter not only the size of the particles, but also the stiffness of the bonds between them. The integration time step was taken to be $0.02t_0$ in the usual LJ reduced units [$t_0=(m\sigma^2_{AA}/\varepsilon_{AA})^{1/2}$], with m being the particle mass. The force due to all the potentials was truncated at the particle distance of $1.55\sigma_{AA}$. The cutoff length was chosen to be at the bottom of the valley between the first and second peaks in the radial-distribution function of the liquid state of the system at a temperature of 0.8 in reduced units (unit is ε_{AA}/k, where k is Boltzmann's constant). All the potentials are shifted so that no discontinuity is left at the cutoff length in the potentials. Although the cutoff length is shorter than the one used conventionally for LJ crystals and produces discontinuities on derivatives of the potentials, it was chosen since the short cutoff length saves much computational time and enables us to reduce the statistical error. Periodic boundary conditions were maintained on all six faces of the cubic block.

The model structure which we call the LJ alloy glass has been constructed in a manner similar to the modified Johnson glass. First, a liquid state of the assembly was attained by a melting at the temperature of 0.8 for 5000 time steps, starting with a fcc crystal randomly occupied by two kinds of particles in a cubic block. The melt at the temperature of 0.8 was well equilibrated because the melting temperature of a LJ elemental crystal is about 0.7,[17] and furthermore our alloying and short cutoff lengths of the potentials decrease the melting temperature. Then the assembly was cooled down to a temperature of 0.275, which is considered to be below the T_g of the system [T_g of a LJ glass is about 0.5 (Ref. 17)], for 1000 time steps. The pressure of the system during this procedure was maintained to be unity (unit is $\varepsilon_{AA}/\sigma^3_{AA}$)

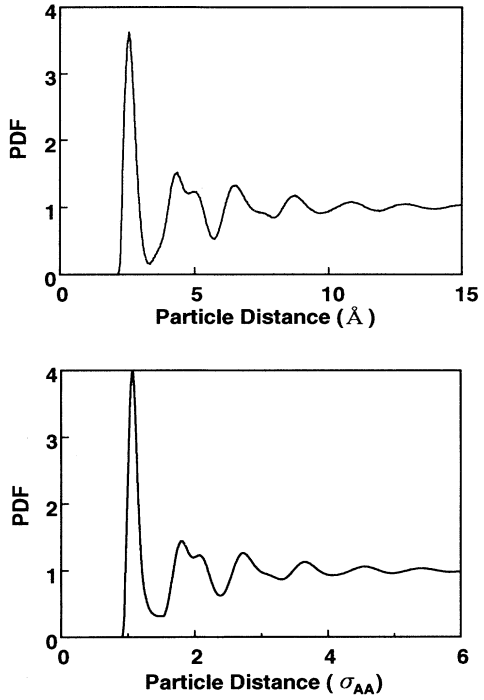

FIG. 1. Pair-distribution function (PDF) of the single-component glass with a modified Johnson potential at 700 K (upper figure) and the total PDF of the two-component glass with the Lennard-Jones potential at a temperature of 0.275 (lower figure).

by changing the boundary conditions and displacing every atom in the block every 100th time step: linear expansion or compression in all directions. Then the assembly was relaxed at the same temperature for 1500 time steps keeping the pressure zero using the same method described above. So as to cause further relaxation, the system was maintained at this temperature for 10 000 time steps without any change of the boundary condition. The shear deformation was applied at a temperature of 0.275 in a manner similar to the modified Johnson glass.

Typical examples of the pair-distribution functions, as described in the next section, of both types of the model glasses are shown in Fig. 1, showing no indication of crystallinity.

III. DIRECTIONAL PAIR-DISTRIBUTION FUNCTIONS AND COORDINATION FUNCTIONS

The averaged structure of glass is most commonly discussed in terms of the radial distribution function (RDF)

$$g(r)=\frac{1}{N}\sum_{ij}\delta(r-r_{ij}) \tag{2}$$

or the pair-distribution function (PDF)

$$p(r)=\frac{1}{4\pi r^2\rho_0}g(r)\ , \tag{3}$$

where N is the number of particles and ρ_0 is the average density. These parameters are, however, nondirectional, while for the discussion of directional deformation, we need to describe directional short-range order. There appears to be no established function to describe the anisotropic structure, but the directional RDF can be defined by an extension of Eqs. (2) and (3) using spherical harmonics,[10]

$$g\left[r,\frac{\mathbf{r}}{r}\right]=\sum_{l,m}\rho_l^m(r)Y_l^m\left[\frac{\mathbf{r}}{r}\right]\ , \tag{4}$$

where Y_l^m is a spherical harmonic and

$$\rho_l^m(r)=\frac{4\pi}{N}\sum_{ij}\delta(r-r_{ij})Y_l^m\left[\frac{\mathbf{r}_{ij}}{r_{ij}}\right] \tag{5}$$

or likewise the directional PDF

$$P\left[r,\frac{\mathbf{r}}{r}\right]=\frac{1}{4\pi r^2\rho_0}g\left[r,\frac{\mathbf{r}}{r}\right]\ . \tag{6}$$

The nondirectional RDF or PDF is thus given by the zeroth-order (isotropic) component of Eq. (4) or (6), respectively.

Although the atomic bonding in network glasses such as silicate glass is well defined, the bonding in glassy metals is ill defined because of the metallic nature of the bonding. It is still possible, however, to distinguish the nearest neighbors from others in metallic glasses, since a deep valley exists between the first and second peaks in the RDF of metallic glasses. Therefore the anisotropy in the atomic positions within the nearest-neighbor shell, which frequently determines properties such as the magnetic property, can be expressed by the directional RDF integrated over the interparticle distance covering the first peak of the RDF, which we will call the directional coordinate function (DCNF),

$$N_c\left[\frac{\mathbf{r}}{r}\right]=\sum_{l,m}D_l^mY_l^m\left[\frac{\mathbf{r}}{r}\right]\ , \tag{7}$$

where

$$D_l^m=\int_0^{\text{cutoff}}\rho_l^m(r)dr\ . \tag{8}$$

The limits of integration in the equation were chosen to be from zero to 3.33 Å for the modified Johnson glass and for the Lennard-Jones alloy glass to be from zero to $1.5\sigma_{AA}$, $1.42\sigma_{AA}$, and $1.35\sigma_{AA}$ for the larger-particle pairs (A-A), the unlike-particle pairs (A-B), or the smaller-particle pairs (B-B), respectively. These cutoffs are at the bottom of the valleys in their RDF's (see Fig. 1). In other words, the DCNF is the averaged number of the nearest neighbors with a certain directional distribution described by spherical harmonics.

Since our creep deformation has uniaxial symmetry and reversal invariance along the z axis, creep-induced anisotropy should appear only on the components with m being equal to zero and l being even. Therefore we study the directional RDF and DCNF ignoring the components with m not equal to zero or odd l. Therefore, Eqs. (6) and (7) become

$$P(r,\theta)=\frac{1}{4\pi r^2\rho_0}\sum_l \rho_l^0(r)Y_l^0(\theta)\ , \tag{9}$$

$$N_c(\theta)=\sum_l D_l^0 Y_l^0(\theta)\ \ (l \text{ even})\ , \tag{10}$$

where θ is the polar angle between the axis along the tensile direction of our creep deformation and the direction of the atomic bond. The term "anisotropic pair-distribution function or anisotropic PDF" will be used to express the difference between the directional PDF's in the tensile stress and its perpendicular directions.

IV. CREEP-INDUCED ANISOTROPY IN THE MODIFIED JOHNSON GLASS

A. Dependence on stress and temperature

The time dependence of the strain under various loads, the creep curves of this assembly at 700 K, is shown in Fig. 2. This temperature is about 200 K below the glass-transition temperature of a modified Johnson glass. The strain sharply increases in the beginning of the period, over about 1500 time steps, partly due to elastic strain. The strain rate then starts to decrease gradually except for the cases with large applied stresses. During the high-stress creep with the stress more than 2% of its shear modulus [shear modulus of a modified Johnson potential glass is 0.7 eV/Å^3 (Ref. 16)], strain rate increases suddenly after about the 5000th time step, indicating inhomogeneous flow occurring due to localized defects of discrete slip bands. The strain rate averaged after the 2500th time step exhibits a strong nonlinear stress dependence and rises sharply beyond a stress of 1% of the shear modulus at all temperatures, as shown in Fig. 3. This stress dependence obeys the well-known thermodynamical flow equation for homogeneous flow in metallic glasses:[3,18–21]

$$\dot{\gamma}=\dot{\gamma}_0 \sinh\left[\frac{\sigma\Omega}{kT}\right]\ , \tag{11}$$

where $\dot{\gamma}$ is strain rate, k is Boltzmann's constant, and Ω is the activation volume. Fitting the stress dependence with this equation, an activation volume of about 25 Å^3 is obtained, which is consistent with the experimental value for iron-based amorphous alloys.[19–21] These aspects of the simulated deformation are consistent with what has been observed in actual macroscopic scale creep-deformation experiments, which suggests that the deformation in this regime is homogeneous even in the scale of the simulation (about $38\times38\times38$ Å^3) except for the high-stress creep.

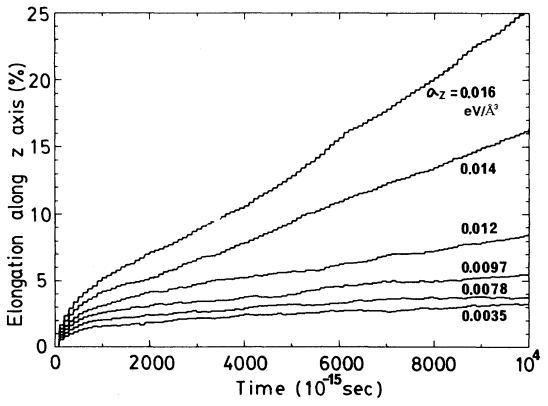

FIG. 2. Time dependence of the elongation along the tensile direction of the simulated creep deformation at 700 K for the modified Johnson glass.

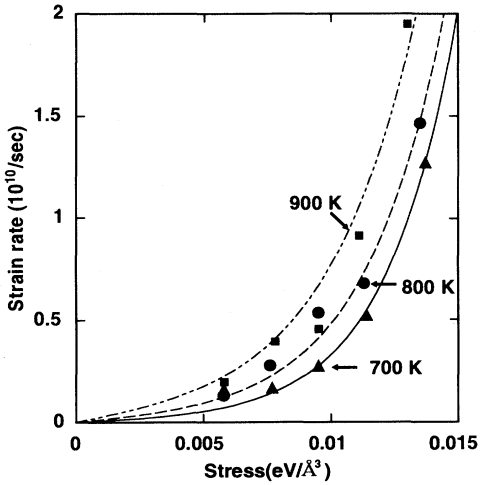

FIG. 3. Stress dependence of the strain rate averaged from 2500 time steps after the start of the creep deformation until the 10 000th time step; lines are the best fits using Eq. (11).

The DCNF's during the creep deformations were then calculated using Eq. (7), at every 100th time step between the 2500th and 10 000th steps and were averaged to reduce the statistical error. A typical example of the stress dependence of the DCNF at 700 K is shown in Fig. 4. The second-order component in the nearest-neighbor shell anisotropy, D_2^0, exhibits linear increase with the stress, while the sixth-order component D_6^0 decreases with the increasing stress and shows a minimum at a stress of about 0.01 eV/Å^3. In contrast, the fourth-order component D_4^0 has almost no stress dependence or shows a slight decrease beyond the stress where D_6^0 shows a minimum. The stress at which the D_6^0 shows a minimum is around 1% of the shear modulus and corresponds to the level of stress at which the creep deformation starts failing to reach its steady state as was mentioned previously. The minimum values of the D_6^0 corresponds to about 10% of the orientational probability of neighboring atoms. The linearly increasing D_2^0 in the modified Johnson glass was found to be due to the elastic strain, by calculating the DCNF after stress release at 300 K. On the other hand, D_6^0 and D_4^0 are anelastic and plastic as will be shown later. These trends clearly suggest that the predominant symmetry of the creep-induced BOA is six-fold.

The temperature dependence of the BOA in the range from 500 to 900 K was explored. Figure 5 shows the temperature dependence of D_6^0 computed during the

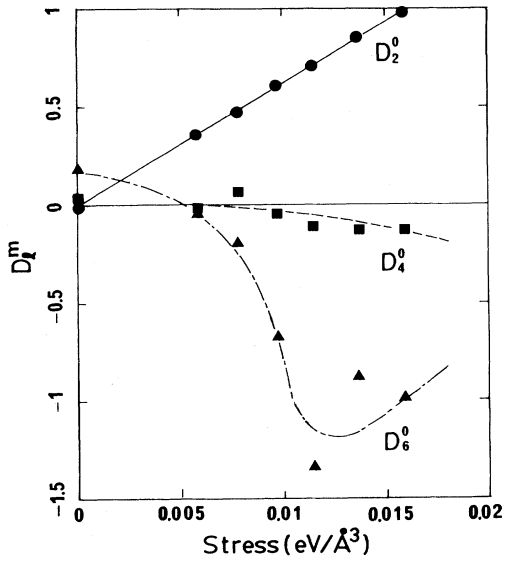

FIG. 4. Stress dependence of the Y_2^0, Y_4^0, and Y_6^0 spherical-harmonic components in the DCNF, D_2^0, D_4^0, and D_6^0, respectively (see text for their definitions), calculated during the creep deformations of the modified Johnson glass at 700 K.

creep as a function of the applied stress. At 500 K the BOA is not caused by creep at least within our computational time and stress scale, exhibiting no stress dependence. However, the stress dependence, and therefore the magnitude of the stress-induced BOA, starts increasing above 600 K. Then the magnitude is likely to show a maximum at around 700 K and decrease at a higher temperature region, although there exists large fluctuations of D_6^0 above 800 K. It should be noted that the temperature at which the highest amount of the BOA is induced

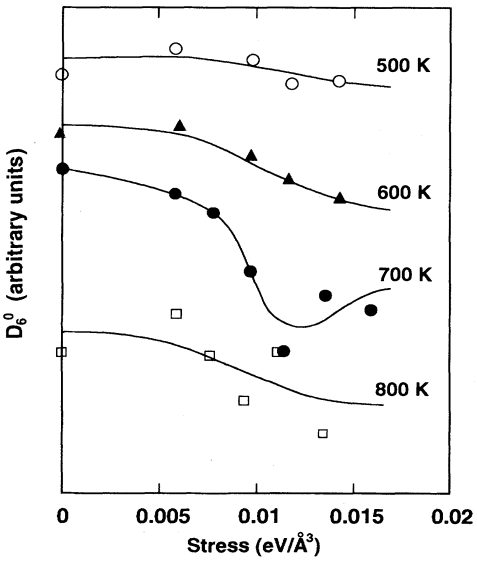

FIG. 5. Stress dependences of D_6^0 calculated during the creep deformation of the modified Johnson glass at several temperatures, showing a maximal stress dependence at 700 K.

is the temperature where many relaxation phenomena in iron-based amorphous alloys take place. That is, these results support the assumption that this anelastic BOA is the origin of the various relaxation phenomena.[11,22]

B. Evolution and relaxation of the BOA and anelasticity

It is interesting to explore how the BOA develops during the creep deformation and if it relaxes at a high temperature. The latter, relaxation of the BOA, should occur if the BOA is not plastic but anelastic. For this purpose a model glass creep deformed at 700 K was quenched down to temperatures ranging from 0 to 600 K, and then the applied stress was unloaded; the quenching period was 100 time steps, and the stress release was performed for 1000 time steps using the reverse fashion of the creep deformation. The anisotropy parameters, including D_2^0, D_4^0, and D_6^0, as well as elongation, were computed during these processes.

Typical examples of the applied stress along the tensile direction D_2^0 and D_4^0 as functions of time are shown in Fig. 6. The behavior of D_2^0 is exactly the same as that of the stress, which confirms that the Y_2^0 component of the anisotropy is elastic; D_2^0 increases suddenly by the loading and relaxes to zero by the unloading. The D_4^0 component, however, does not relax at all after unloading at all the relaxation temperatures simulated, although it develops quickly and saturates after loading as if it were elastic. The D_4^0 component, therefore, exhibits strong plastic characteristics.

Figure 7 shows the evolution and relaxations of D_6^0 at several temperatures; the stress was applied during the

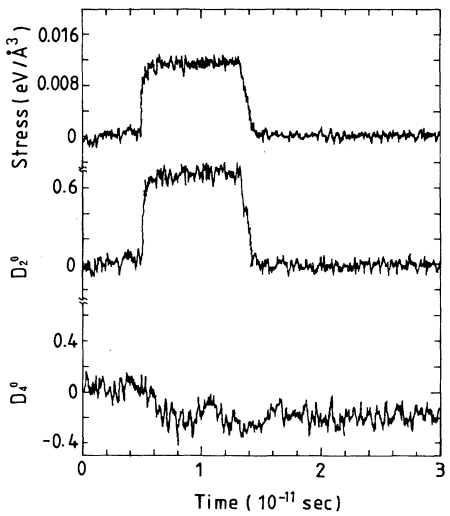

FIG. 6. Time evolutions of the applied stress, D_2^0, and D_4^0 during the creep deformation and the subsequent unloading and relaxation processes for the modified Johnson glass. The stress was applied after keeping the model glass unstressed for 5000 time steps until the 13 000th time step at 700 K, and then the stress was unloaded after quenching to 500 K; the quenching and unloading were performed for 200 and about 800 time steps.

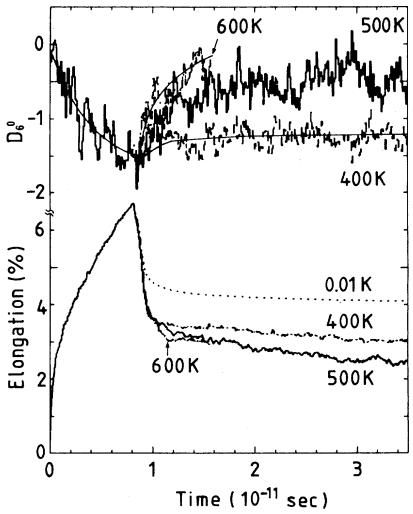

FIG. 7. Time evolution of D_6^0 and elongation along the tensile direction during the creep deformation at 700 K and the subsequent unloading and relaxation processes. These processes are the same as those shown in Fig. 5; the process of keeping the model glass unstressed for 5000 time steps is not illustrated in this figure.

period from the 5000th to 13 000th time step at 700 K as was shown in Fig. 6. During the creep, D_6^0 develops gradually and appears to saturate at the end of the creep. Unlike D_4^0, D_6^0 does show relaxation; i.e., the Y_6^0 component of the anisotropy is anelastic. Although it relaxes only slightly at 400 K, most of the creep-induced part of D_6^0 is released at 500 and 600 K within our time scale of simulation. D_6^0 rises quickly in the beginning of the relaxation process, and the rate of increase decreases monotonously as is expected for thermodynamical relaxation processes occurring against an activation barrier; at 600 K, the relaxation is observed to occur even during unloading.

It should be noted that the relaxation of D_6^0 at 500 K appears to saturate to a somewhat smaller value than at 600 K. D_6^0 fluctuates around -0.45 at 500 K even 25 000 time steps after unloading, whereas it quickly reaches about -0.2 at 600 K. It is impossible to fit the curve at 500 K using one exponential function even if we assume that it is relaxing toward the value of -0.2; it is also likely that the saturation of D_6^0 after the initial sharp rise occurs even at 400 K. This behavior indicates that the relaxation occurs not with a single activation energy, but with a wide distribution of the energies.

It is noteworthy that the relaxation of the sixth-order component occurs not toward zero, but toward a point before the creep, i.e., an anisotropic state frozen in during the quenching from its liquid state. As the temperature of the model glass drops from above the melting point, D_6^0 was observed to fluctuate widely around zero above 1500 K and the fluctuation freezes during the subsequent quench toward the glass-transition temperature. Consequently, D_6^0 remains a certain nonzero value below the temperature, fluctuating around it. Such "frozen-in" anisotropy is the largest on the sixth-order component among the observed three components; the anisotropy on the fourth is one order magnitude smaller than that for the sixth and that for the second is negligible within the statistical error of this simulation. This anisotropy on the sixth-order component sometimes reaches to about the half of the maximum creep-induced anisotropy observed. The primary difference between the frozen-in and creep-induced anisotropies is that the frozen-in anisotropy does not relax below the glass-transition temperature, but the creep-induced one does within our simulation time scale.

The large anelasticity was observed during the relaxation, as shown in Fig. 7. The time-dependent recovery of the strain occurs at all the relaxation temperatures similarly to D_6^0. At 0.01 K, the strain falls linearly during unloading and then starts departing from the linearity after about 1.5% of recovery. This linear recovery is due to elastic strain and is consistent with the applied stress of about 1.5% of the shear modulus. The strain continues to decrease gradually after the departure from the linearity, showing that a part of the anelastic recovery possesses a vanishingly small activation energy. At higher temperatures the sharp decrease during unloading exceeds the strain of 1.5%, which is expected to be the limit of elastic recovery as mentioned above. Therefore, at higher temperatures, the time scale for a part of the anelastic relaxation is considered to be small compared to the time scale for unloading, again indicating a broad distribution of activation energy existing. At 600 K, the anelastic recovery exhibits a saturation 6000 time steps after loading in a similar manner to the relaxation of D_6^0 at the same temperature. The overall anelastic recovery increases with increasing the temperature to 500 K and reaches about 2% of contraction and 50% of creep deformation and decreases again at 600 K within our observation time. Thus, although those anelastic parts of the recovery curves resemble D_6^0 relaxation curves, the anelastic recovery is not linear with the recovery of D_6^0.

V. CREEP-INDUCED ANISOTROPY IN LENNARD-JONES ALLOY GLASS

The time-strain (creep) curves for the two-component Lennard-Jones glass, shown in Fig. 8, were obtained by the procedure described previously. They are very much similar to the creep curves for the single-component glass shown in Fig. 2. After a period of 2500 time steps, the strain rate appears to become relatively constant, although there exists a large fluctuation of the strain due to the statistical error of σ_z. Therefore the anisotropy parameters D_l^0's during the creep deformation were calculated every 10th time step after the 2500th step to the 10 000th step and were averaged, as performed for the modified Johnson glass. The stress dependences of the D_l^0's shown in Fig. 9 considerably resemble those of the single-component glass shown in Fig. 3. The second-order component D_2^0 depends linearly on the applied stress, whereas D_6^0 shows a minimum at the stress of around 0.2, which is about 1% of the shear modulus of a LJ glass [the shear modulus of a LJ glass is about 30 (Ref. 17)]. In contrast to these components, D_4^0 stays at a

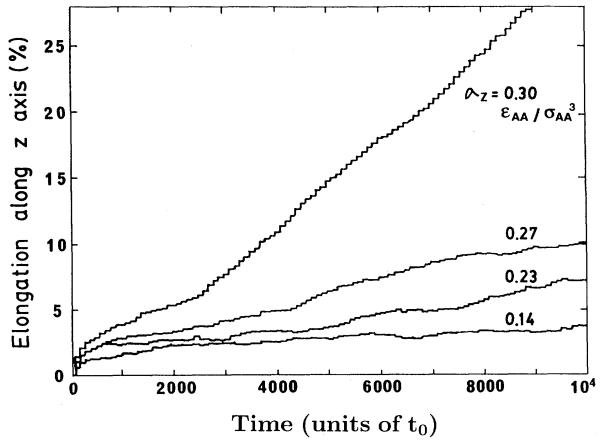

FIG. 8. Typical time dependence of the elongation along the tensile direction of the simulated creep deformation for the two-component LJ glass.

slightly negative value, which is considered the anisotropy quenched in from the liquid state of the model structure and is independent of σ_z. These trends again suggest that the Y_2^0 component is elastic and that the anelastic part of the anisotropy, therefore the BOA, induced by the creep deformation is the Y_6^0 component.

To confirm this point further, the anisotropy within stress-free states after the creep deformation was computed. For this purpose a creep-deformed assembly was quenched to a temperature of 0.1 and then the remaining stress was released; the quenching period was 100 time steps and unloading was performed for 1500 time steps using the reverse fashion of the creep deformation. This process was applied for 15 creep-deformed states that were sampled every 500th time step after the 2500th step to the 10 000th step during the creep deformation. Then the directional RDF's for these relaxed states were computed and averaged. A typical example of the total DCNF including all the kinds of atomic pairs, and therefore the existence probability of the nearest-neighbor atoms, is shown as a histogram in Fig. 10 along with the total DCNF before the deformation. After the deformation it deviates significantly from the averaged coordination number of 12.8 as a smooth function of θ, the polar angle away from the tensile direction, while it only fluctuates within statistical noise before the deformation. The anisotropy retains as much of the Y_6^0 component as that during the corresponding deformation shown in Fig. 9, whereas the second-order component vanishes during the unload; the dashed line in the figure is a function consisting of the Y_0^0, Y_2^0, Y_4^0, and Y_6^0 components deduced from the histogram; these components correspond to D_0^0, D_2^0, D_4^0, and D_6^0, respectively. This result clearly demonstrates that the Y_6^0 component predominates the anelastic anisotropy.

In multicomponent glasses compositional short-range order (CSRO) can be directional and can contribute to the anisotropy of its properties.[11] In order to see if mechanical deformation could induce such an anisotropy, the directional CSRO, the change in the compositionally resolved partial DCNF's due to deformation, was calculated for the stress-released states mentioned above at a temperature of 0.275. The results are shown in Fig. 11. Although there were more fluctuations in the partial DCNF's due to poorer statistics compared to the total DCNF, dominant Y_6^0 components were found in all of the partial DCNF's. Moreover, no clear difference between the ratios of these Y_6^0 components to the corresponding

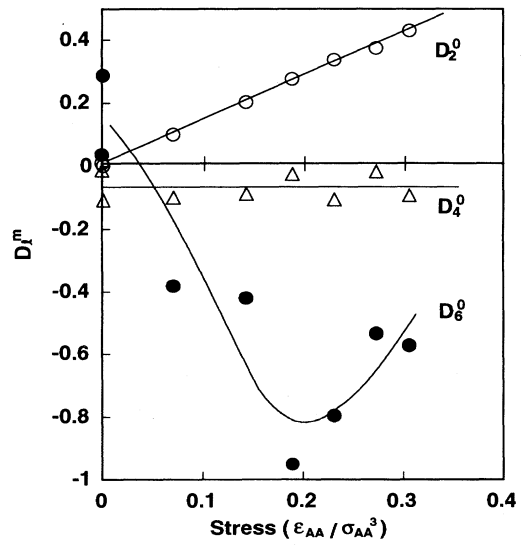

FIG. 9. Stress dependence of D_2^0, D_4^0, and D_6^0 calculated during the creep deformations of the LJ model glass.

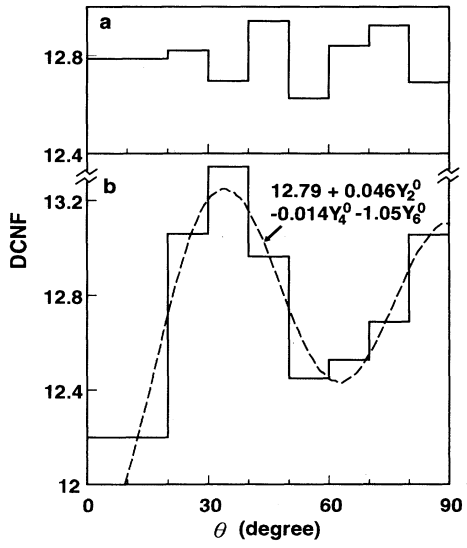

FIG. 10. Total DCNF's (a) calculated for the LJ model glass without deformation and (b) calculated for the unloaded LJ glass after creep deformation with an averaged stress of 0.19 (histograms). The dashed line shows the function consisting of the Y_2^0, Y_4^0, and Y_6^0 spherical-harmonic components deduced from the latter histogram. The former DCNF was obtained by calculating DCNF's every 10 time steps for 10 000 time steps and averaging them (see text for the calculation procedure of the latter DCNF).

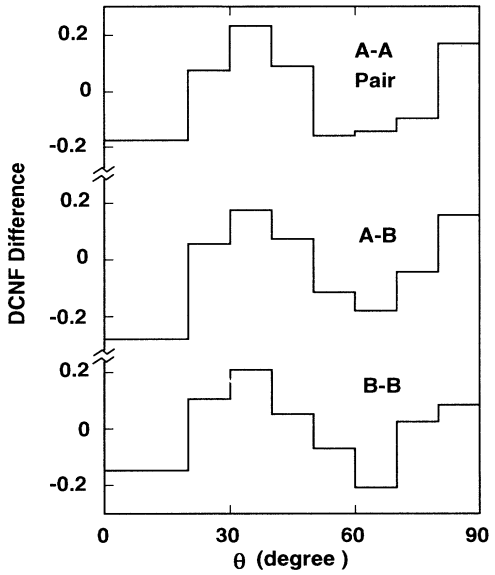

FIG. 11. Difference between the compositionally resolved partial DCNF's calculated for the unloaded LJ glass after creep deformation with an averaged stress of 0.19 and calculated without deformation; calculation procedures for them are the same as those for the total DCNF's shown in Fig. 10.

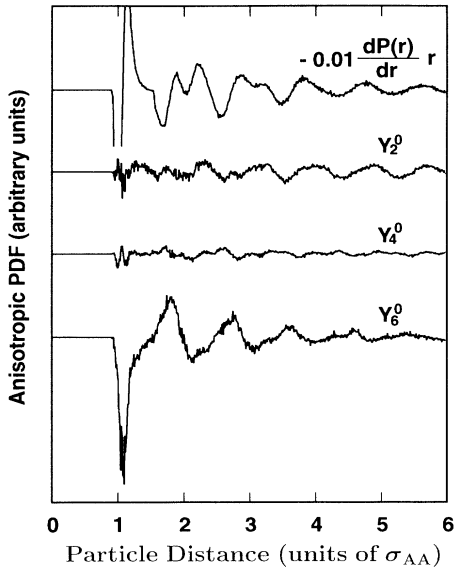

FIG. 12. Derivative of the total PDF and the Y_2^0, Y_4^0, and Y_6^0 spherical-harmonic components of the total anisotropic PDF calculated for the stress-released state after the creep deformation with an averaged stress, $\sigma_z = 0.27$.

partial coordination numbers was found. Thus, for this particular set of interatomic potentials, the creep deformation does not produce directional CSRO, but activates predominantly the directional topological short-range order (TSRO),[11] i.e., the BOA.

We have so far been concerned only with the structural anisotropy within the first nearest neighbors. It is of further interest to look at how the BOA in the nearest-neighbor shell would affect the atoms beyond the first-nearest-neighbor shell, because experimentally creep deformation is known to result in a uniform long-range strain in the atomic structure.[10] We calculated the Y_2^0, Y_4^0, and Y_6^0 components of the anisotropic PDF for the stress-released state of the creep-deformed assembly with the averaged stress $\sigma_z = 0.27$, as shown in Fig. 12; all of the atomic pairs were included regardless of the chemistry. The important features of the medium-range anisotropy described in Ref. 10 were again found in the Y_2^0 and Y_6^0 components in the anisotropic PDF. The Y_2^0 component is negligible within the first-nearest-neighbor shell; however, this component increases with increasing particle distance. In contrast with the Y_2^0 component, the Y_6^0 component is large within a distance of about $3\sigma_{AA}$, while it dies out beyond this distance. The behavior of the Y_2^0 component in the medium-range distance is well characterized by the uniform elongation of about 1% strain along the Z axis, which is consistent with experiment.[10] The Y_2^0 component beyond a distance of $3\sigma_{AA}$ is very close to the derivative of the PDF of this assembly, $-\varepsilon[dp(r)/dr]r$ ($\varepsilon = 0.01$), shown in Fig. 12. Note that the assembly for this anisotropic PDF calculation is free from macroscopic stress. The Y_6^0 component in the medium-distance range, however, has almost the opposite sign to that derivative. It is also noteworthy that the anisotropic PDF has an almost negligible Y_4^0 component in any distance range.

VI. DISCUSSION

A. Local bond-orientation order

Since a stress tensor has the $l = 2$ symmetry,[23] it is natural to expect that the structural anisotropy induced by stresses will have the same symmetry. Indeed, the elastic part of the anisotropy was found to have $l = 2$ symmetry, represented by D_2^0. Somewhat surprisingly, the structural anisotropy associated with the anelastic strain has $l = 6$ symmetry. However, this is not all that surprising if we consider the nature of the bond-orientational order. This may be best illustrated by the case of a two-dimensional structure.

The bond-orientational order (BOO) in the two-dimensional assembly of atom is characterized by[24]

$$Q_6 = \frac{1}{N}\sum_{ij} \langle\langle e^{i6\theta_{ij}} \rangle\rangle , \tag{12}$$

where the ith and jth atoms are the nearest neighbors to each other and θ_{ij} denotes the orientation of the bond connected between the ith and jth atoms relative to the external coordinates. The BOO becomes long range either in the close-packed (triangular) crystalline phase or in the hexatic phase,[24] but is only short range in the liquid phase. In the liquid phase, the average BOO is zero in equilibrium, but by applying external stress it is conceivable that the local order is temporarily biased so that the average BOO is not zero. In such a biased structure, a triangle formed by three atoms will be found more often in one or the other of the two in Fig. 13, resulting in

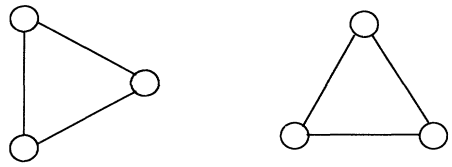

(a) (b)

FIG. 13. Two extreme orientations of a triangular atom cluster, with (a) $Q_6=1$ and (b) $Q_6=-1$.

the BOA state. The transition from one state to the other can be achieved by the bond exchange shown in Fig. 14, where one bond is annihilated while another is created as a result of external stress. Although the angle between the annihilated and created bonds is 90°, the change in the bond orientations is 30°, resulting in a change in Q_6.

The concept of BOO was generalized to three dimensions by Steinhardt, Nelson, and Ronchetti, who suggested that the liquidlike state with long-range BOO, a three-dimensional analog of the hexatic phase, may be possible.[25] While their suggestion remains controversial,[26] their analysis of the BOO in the three-dimensional liquid is directly relevant to our analysis. The relevant order parameter is, then,

$$Q_l^m=\frac{1}{N}\sum_{ij}\left\langle\left\langle Y_l^m\left[\frac{\mathbf{R}}{r}\right]\right\rangle\right\rangle , \tag{13}$$

which is equivalent to D_l^m except for the factor 4ρ, by Eqs. (5) and (8). They pointed out that the dominant symmetry component in the three-dimensional liquid with strong short-range order is sixfold, described by Eq. (13). Such a local order is likely to be associated with the local icosahedral clusters, which can, in a single-component system, exist only in the noncrystalline solids, and consequently this analysis led to the recognition of the quasicrystalline state.[27]

B. Bond exchange and mechanical deformation

In analogy to the two-dimensional liquid, it is entirely possible that an external field leads to the polarization of the $l=6$ local BOO, and our MD simulation proves that thermomechanical deformation in fact results in such a local polarization. The mechanism will still be the bond exchange shown in Fig. 14, although the actual atomic configurations involved in the deformation may be three-dimensionally distorted. By a computer simulation of the deformation of metallic glasses, it has been shown that the nonelastic strain is proportional to the number of incidents of bond exchange.[28] The total shear strain ε_t is given by

$$\varepsilon_t=\varepsilon_{\rm el}+\varepsilon_{\rm nonel} , \tag{14}$$

where $\varepsilon_{\rm el}$ is the elastic strain,

$$\varepsilon_{\rm el}=\frac{\tau}{2G_0} , \tag{15}$$

where τ is the applied shear stress and G_0 is the ideal shear modulus for uniform deformation without bond exchange, which can be calculated as the second derivative of the total energy with respect to the uniform strain,[23] and $\varepsilon_{\rm nonel}$ is the nonelastic strain given by

$$\varepsilon_{\rm nonel}=\alpha\frac{N_r}{N} , \tag{16}$$

$$\alpha=0.078\approx\frac{1}{N_c} , \tag{17}$$

where N_r is the number of bond rearrangements, cut or formed, and N is the total number of atoms. The coefficient α was found to be very close to the inverse of the coordination number N_c. Since the total number of bonds is approximately preserved even during deformation, the number of bonds cut is about equal to the number of bonds formed, thus justifying the concept of bond exchange.

A local bond exchange is anelastic, since the local deformation as in Fig. 14 will produce a strain field around it and create a back stress due to the environment. However, when the number of the locally deformed sites exceeds the percolation threshold, the back stress will be macroscopically relaxed, and the deformation will become *plastic*. The critical strain for the plastic deformation to start, ε_c, is then given by

$$\varepsilon_c=\alpha c_p , \tag{18}$$

where c_p is the percolation limit (≈ 0.15 for the DRP structure[29]). Thus we obtain

$$\varepsilon_c\approx 0.012 , \tag{19}$$

which is very close to the point where D_6^0 reaches the minimum and the plastic deformation starts, for both the single- and two-component glasses. When plastic flow occurs, the BOA is likely to be randomized and reduced. Thus the BOA is maximum just at the critical strain for the start of the plastic flow.

The amount of BOA induced depends also on temperature and is maximum at about 80% of T_g. This is because the bond rearrangement is a thermally activated process. At low temperatures the activation is kinetically hindered, i.e., very slow, while at high temperatures too many bond rearrangements would occur leading to plastic flow. Thus the temperature at which the BOA is maximum should depend upon the time scale of measure-

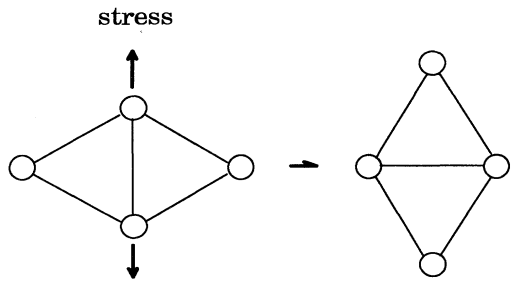

FIG. 14. Schematic representation of the atomic rearrangement under a stress.

ment. Since the time scale used in the MD simulation is very short, the maximum is expected to occur at somewhat lower temperatures in the real experiments.

VII. CONCLUSIONS

Thermomechanical (creep) deformation of metallic glasses was simulated by molecular dynamics for single-component model glass with a modified Johnson potential and for a two-component glass with a Lennard-Jones potential. The results for both model glasses were almost identical to each other and led us to the following conclusions.

(1) The creep deformation results in a directional topological short-range order, with a dominant Y_6^0 spherical harmonic component of the local bond-orientational order. Thus the bond-orientational anisotropy (BOA) induced by creep has sixfold ($l=6$) symmetry. Directional compositional short-range order was not induced within our statistical error.

(2) The induced BOA exhibits a maxima with respect to both applied stress and temperature. The maximum appears at the tensile stress of about 1% of the shear modulus in the stress dependence of the BOA near the onset of plastic deformation and likewise at a temperature of about 80% of the glass-transition temperature.

(3) The BOA relaxes with a broad distribution of activation energies, and during this relaxation, a partial recovery of the creep deformation, i.e., anelastic recovery, takes place.

(4) The Y_6^0 component of the BOA decays quickly with distance beyond the second-nearest neighbor, and instead the Y_2^0 component of the BOA characterized by a uniform elongation appears in this range.

(5) These activations and relaxations of the Y_6^0 BOA and anelasticity can be explained by local rearrangements of atomic bonds. The depolarization is driven by the back stress in the matrix surrounding the polarized region.

ACKNOWLEDGMENTS

The authors are grateful to Dr. X. Yan for helpful discussion and comments and Dr. E. Marshal for assisting in the computations. This research was supported by Sumitomo Metal Industries.

*Present address: Advanced Technology Research Laboratories, Sumitomo Metal Industries, Ltd., Amagasaki 660, Japan.

[1]R. Maddin and T. Masumoto, Mater. Sci. Eng. **9**, 153 (1972).
[2]H. Fujimori, in *Amorphous Metallic Alloys,* edited by F. E. Luborsky (Butterworths, London, 1983), p. 300.
[3]A. S. Argon, Acta. Metall. **27**, 47 (1979).
[4]A. S. Argon and H. Y. Kuo, J. Non-Cryst. Solids **37**, 241 (1980).
[5]A. S. Argon and H. Y. Kuo, Mater. Sci. Eng. **39**, 101 (1979).
[6]D. Deng, A. S. Argon, and S. Yip, Philos. Trans. R. Soc. London A **329**, 613 (1989).
[7]O. V. Nielsen and H. J. V. Nielsen, Solid State Commun. **35**, 281 (1980).
[8]O. V. Nielsen and H. J. V. Nielsen, J. Magn. Magn. Mater. **22**, 21 (1980).
[9]H. R. Hilzinger, in *Proceedings of the 4th International Conference on Rapidly Quenched Metals,* edited by T. Masumoto and K. Suzuki (Japan Institute of Metals, Sendai, 1982), Vol. 2, p. 791.
[10]Y. Suzuki, J. Haimovich, and T. Egami, Phys. Rev. B **35**, 2162 (1987).
[11]T. Egami, in *Amorphous Metallic Alloys* (Ref. 2), p. 100.
[12]M. Hirscher, T. Egami, and E. E. Marinero, J. Appl. Phys. **67**, 4932 (1990).
[13]X. Yan, M. Hirscher, T. Egami, and E. E. Marinero, Phys. Rev. B **43**, 9300 (1991).
[14]T. Egami and V. Vitek, in *Amorphous Materials,* edited by V. Vitek (Metal Society of AIME, Warrendale, PA, 1983), p. 127.
[15]R. A. Johnson, Phys. Rev. **134**, 1329 (1964).
[16]S.-P. Chen. T. Egami, and V. Vitek, Phys. Rev. B **37**, 2440 (1988).
[17]H. Hsieh and S. Yip, Phys. Rev. Lett. **59**, 2760 (1987).
[18]F. Spaepen, Acta Metall. **25**, 407 (1977).
[19]A. I. Taub, Acta Metall. **28**, 633 (1980).
[20]D. G. Ast and D. J. Krenifsky, J. Mater. Sci. **14**, 287 (1979).
[21]F. Spaepen and A. I. Taub, in *Amorphous Metallic Alloys* (Ref. 2), p. 231.
[22]T. Egami, Rep. Prog. Phys. **47**, 1601 (1984).
[23]T. Egami and D. Srolovitz, J. Phys. F **12**, 2141 (1982).
[24]D. R. Nelson and B. I. Halperin, Phys. Rev. B **19**, 2457 (1979).
[25]P. J. Steinhardt, D. R. Nelson, and M. Ronchetti, Phys. Rev. B **28**, 748 (1983).
[26]R. M. Ernst and S. R. Nagel, Phys. Rev. B **43**, 8070 (1991).
[27]D. Levine and P. J. Steinhardt, Phys. Rev. Lett. **53**, 2477 (1984).
[28]Y. Suzuki and T. Egami, J. Non-Cryst. Solids **75**, 361 (1985).
[29]H. L. Fitzpatrick, R. B. Malt, and F. Spaepen, Phys. Lett. **47A**, 207 (1974).